Nikolai A. POKLONSKI[1], Nikolay I. GORBACHUK[1], Anna V. ERMAKOVA[1], Mariya I. TARASIK[1], Sergey V. SHPAKOVSKI[2], Viktor A. FILIPENIA[2], Viktor A. SKURATOV[3], Andreas WIECK[4], Tomasz N. KOŁTUNOWICZ[5]

Belarusian State University, Minsk, Belarus (1), JSK Integral, Minsk Belarus (2), Joint Institute for Nuclear Research, Dubna, Russia (3), Ruhr-Universitaet Bochum, Bochum, Germany (4), Lublin University of Technology, Lublin, Poland (5)

Impedance of reverse biased diodes irradiated with krypton ions with energy of 250 MeV

Abstract. *The p^+n-junction silicon diodes irradiated with krypton ions with the energy of 250 MeV were studied. The distance δ between the p^+n-junction boundary and calculated maximum in the distribution of the primary vacancies was about 26.4 μm. It was shown that transformations of a complex plane plot of the electric modulus at the increased reverse bias take place due to a change in the impedance ratio Z_L/Z_J of the irradiation damaged layer Z_L to space charge region Z_J as well as due to changes in the electron population of the energy levels of irradiation-induced defects.*

Streszczenie. *Przebadano diody krzemowe o typu p^+n naświetlane jonami kryptonu o energii 250 MeV. Odległość δ między granicą złącza p^+n i obliczonym maksimum w rozkładzie wakatów pierwotnych wyniosła około 26,4 μm. Wykazano, że przekształcenia zespolonej płaszczyzny modułu elektrycznego przy zwiększonej polaryzacji zaporowej złącza mogą nastąpić pod wpływem zmiany stosunku impedancji Z_L/Z_J warstwy zdefektowanej promieniowaniem Z_L do impedancji obszarów z ładunkiem przestrzennym Z_J, jak również ze względu na zmiany w koncentracji elektronów na poziomach energetycznych defektów powstałych poprzez promieniowanie. (**Impedancja diod spolaryzowanych zaporowo napromieniowanych jonami kryptonu o energii 250 MeV**).*

Keywords: Ion irradiation, p^+–n junction diode, impedance.
Słowa kluczowe: promieniowanie jonowe, dioda o złączu p^+n, impedancja.

Introduction

Radiation technologies have found a wide use in semiconductor industry. Capacitance methods are most frequently applied for estimation of the semiconductor layer parameters (e.g., dopant concentration and its distribution profile, presence and concentration of the electrically active defects) in studies of the semiconductor barrier structures. They are extensively used to control the technological processes. However, when diodes have a high-resistance base [1, 2] or when the base contains high concentrations of the centers having their energy levels deep within the bandgap [2-5], measurements of the capacitance demand thorough analysis of the results and require additional calculations [5-7]. Also, there is a need in separation of the contributions into the measured impedance (capacitance) of a diode made by the space charge region, diode base, and by the delay in recharging of the deep-level defects. Upon high-energy ion irradiation, the radiation defects are concentrated within a layer of the finite thickness. Because of this, in addition to the above-mentioned aspects, a contribution of this layer into the diode impedance should be taken into consideration too.

The aim of the work is to study the effect of the layer of irradiation-induced defects formed by irradiation with high-energy krypton ions on the frequency dependences of impedance of the p^+n-junction silicon diodes.

Experimental technique

The diodes were manufactured on uniformly phosphorous doped single-crystalline silicon wafers (thickness 460 μm, (111) orientation) grown by crucibleless zone melting. Wafers resistivity was equal to 90 Ω×cm, phosphorous concentration was 5×10^{13} cm^{-3}. The p^+-type region was formed by boron ion implantation with the energy 60 keV and dose 90 μC/cm^2 (5.6×10^{14} cm^{-2}) using a "Vesuvius-3M" ion implanter with subsequent annealing of the defects and with the dopant drive-in in an oxidizing atmosphere at 1100°C for a period of 50 min. The boron diffusion process was simulated with the use of the Process Wizard 1D Program [8]. The distribution profile for the difference $|N_A - N_D|$ in acceptor and donor concentrations based on the results obtained during simulation of the technologicval process is shown in Fig. 1 (curve *1*). A depth of the p^+n-junction was controlled by the results of chemical etching of the spherical metallographic section and found to be $x_j \approx 3.5$ μm. This value is in a satisfactory agreement with the calculations. Being estimated from measurements of the capacitance-voltage characteristics at $U = 0$, a thickness of a double electric layer of the p^+n-junction in the virgin diodes was about 4.5 μm. An active area of the p^+n-junction was 4.41 mm^2. To create the ohmic contact to the base, phosphorous ions (energy 75 keV and dose 500 μC/cm^2 (3.1×10^{15} cm^{-2})) was implanted into the nonplanar side of a silicon wafer. The contacts were formed by Al sputtering with subsequent fusing at the temperature 475°C in nitrogen atmosphere (Al layer thickness at the contact to the p^+-region was 1.5 μm).

The diodes were irradiated with krypton ions. Irradiation energy was 250 MeV, fluence was 10^9 cm^{-2}. The implantation direction was perpendicular to the p^+n-junction plane from the p^+-region. Fig. 1 (curve *2*) shows the distribution profiles for the primary radiation vacancies calculated using the TRIM Program [9]. The distance δ between the p^+n-junction boundary ($N_A = N_D$, disregarding compensation of the dopant by radiation defects) and maximum in the distribution of the primary vacancies was found to be 26.4 μm.

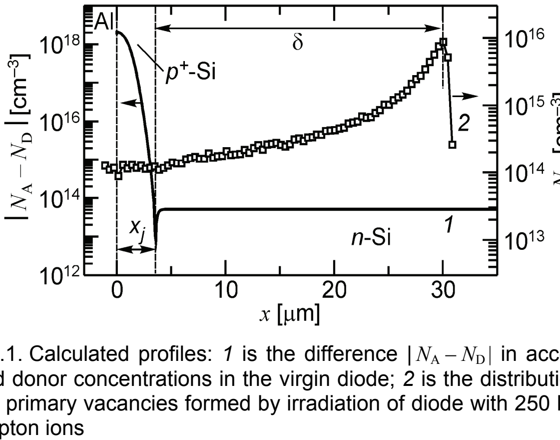

Fig.1. Calculated profiles: *1* is the difference $|N_A - N_D|$ in acceptor and donor concentrations in the virgin diode; *2* is the distribution of the primary vacancies formed by irradiation of diode with 250 MeV-krypton ions

The static current-voltage characteristics were registered according to a standard procedure using an HP4156B program-analytical system.

Both the real Z' and the imaginary Z'' parts of impedance $Z = Z' + iZ'$ were measured at room temperature with the use of Agilent E4980A and Agilent 4285A LCR-meters. The studies were performed in the alternating-current frequency f range from 20 Hz to 30 MHz. The sinusoidal voltage amplitude was below 40 mV.

Experimental results and discussion

Fig. 2 (curve *1*) presents the reverse current I_r as a function of the reverse bias voltage U_r for the diodes irradiated with high-energy krypton ions with the fluence of 10^9 cm^{-2}. As it is seen, the function has several sections differing in their slopes. Consequently, the dependence of the differential conductance $G = dI_r/dU_r$ of the diodes on the reverse bias voltage U_r is a nonmonotonic function. The maximum of $G(U_r)$ is observed at $U_r \approx -14.3$ V.

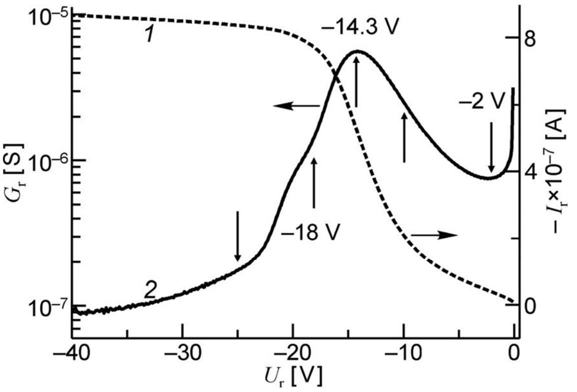

Fig.2. Reverse current I_r (*1*) and differential conductance $G = dI_r/dU_r$ (*2*) as functions of the reverse bias voltage U_r

The complex electric modulus $M = i\omega C_0 Z$ (C_0 is the capacitance of a vacuum capacitor with the geometry identical to that of the sample studied) is a quantity reciprocal to the complex permeability. In some cases (see, e.g., [10, 11]) the representation of the measured frequency dependences of impedance as the plots of electric modulus in the complex plane enables one to reveal the features in the alternating current conduction for heterogenic systems and semiconductor devices.

Fig. 3 shows a plot of the quantity M^* proportional to the complex electric modulus $M^* = M/C_0 = \omega(-Z'' + iZ')$ at different bias voltages. By the physical mean M^* is a quantity reciprocal to the diode capacitance. For simplicity and for uniformity of the terms with [10], the quantity M^* will be further referred to as the complex electric modulus. It is seen that, as the space charge region is widened, the form of plots for the complex electric modulus changes dramatically. For $U_r = 0$ the plot of M^* clearly reveals the presence of four sections (arcs). In Fig. 3 they are denoted by Roman numerals from I to IV. The low-frequency ($f < 3$ kHz) arc I is determined by the space charge region. It grows with an increase in the reverse voltage from 0 to 10 V. The intersection point of the arc extrapolation with the axis $-\omega Z''$ is shifted to the greater values. This is associated with a decrease in the barrier capacitance. A small high-frequency section (arc IV, $f > 5$ MHz) is determined by the diode base layer which left intact during ion implantation. A form of the arc IV is actually independent of U_r. The most significant changes in M^* are observed in the frequency range from 3 kHz to 5 MHz. Two arcs (II and III) in the curve of M^* are considerably reduced as the absolute value of bias voltage is growing to become practically indistinguishable for $|U_r| > 18$ V in the scale of Fig. 3.

Fig. 4 shows (Fig. 4*a*) the electric modulus plot in complex plane for $|U_r| > 25$ V and its scaled up fragment (Fig. 4*b*). Two deformed arcs are clearly visible.

Fig. 5 presents scaled up fragments of the complex electric modulus plots associated with the arcs II and III. The plots is based on the results of measurements at the reverse bias voltages $|U_r| > 14.3$ V. As it is seen, transformations in the third and fourth arcs in the plots of M^* are observed over the whole range of U_r studied.

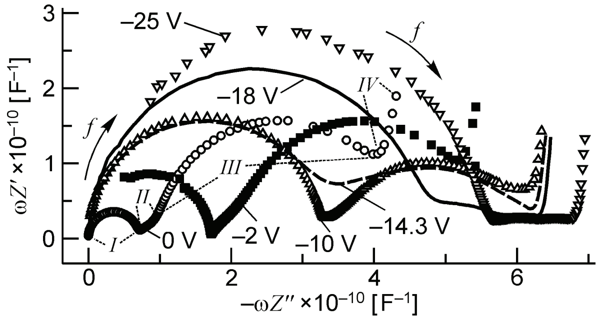

Fig.3. Plots of the electric modulus in the complex plane. Values of the reverse bias voltage U_r used in measurements are marked in Fig.2 by arrows

High-energy ion implantation leads to the formation of a layer of radiation defects buried within the diode base. A maximum in the defect distribution is found at the depth somewhat smaller than the average projected range of implanted ions [12]. As the distance $\delta \approx 26.4$ μm is considerably greater than the thickness of the space charge layer for $U_r = 0$, then the diodes under study in fact represent a multilayer structure consisting of the space charge region, irradiation damaged layer, and undamaged layer of the diode base. The impedance Z of the diodes is a sum of the three components $Z = Z_J + Z_L + Z_B$, where Z_J is the impedance of the space charge region, Z_L is the impedance of the irradiation damaged layer, Z_B is impedance of the diode base. The frequency dependences of Z_J and Z_L in turn may be influenced by the delay in recharging of deep level defects [11, 13]. The layer thickness and impedances Z_J, Z_L, Z_B may be varied depending on the value of U_r. The space charge region is expanded in depth of the base as the reverse bias is increased. The process of expansion involves the irradiation damaged layer leading to the increased reverse currents and greater differential conductance of the diodes (see Fig. 2). When the layer of irradiation-induced defects is completely entrapped into the space charge region, further increase of the reverse currents is slowing down and the values of G in their order of magnitude are approaching the conductance of nonirradiated diodes.

As it follows from Fig. 2, the effect of irradiation-induced defects becomes considerable for $|U_r| \geq 2$ V. For $|U_r| = 25$ V, actually the whole irradiation damaged layer appears within the space charge region. In this way the transformations observed on the curves for M^* (transformations of the arcs *I–III*) when the absolute value of U_r increases from 2 V to 25 V are associated with propagation of the space charge region and with following gradual reduction of the irradiation damaged layer, i.e., actually with the decrease in Z_L.

From Figs. 3 and 5 it follows that the transformations in the plots of M^* are observed even when the whole irradiation damaged layer is entrapped by the space charge region. In this case the transformations are induced by the changes in the electron populations of energy levels caused by a change in the position of a quasi-Fermi level with respect to the level of irradiation-induced defects as the value of $|U_r|$ is further growing.

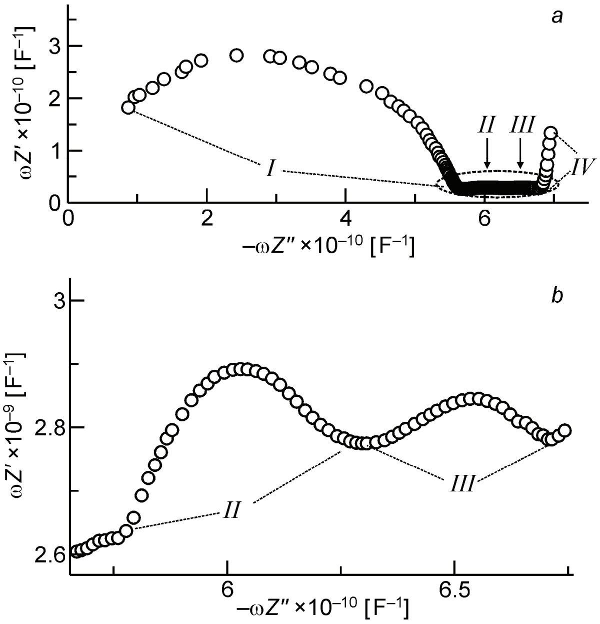

Fig. 4. Plot of the electric modulus in the complex plane (*a*) for $|U_r| = 25$ V and its scaled up fragment (*b*)

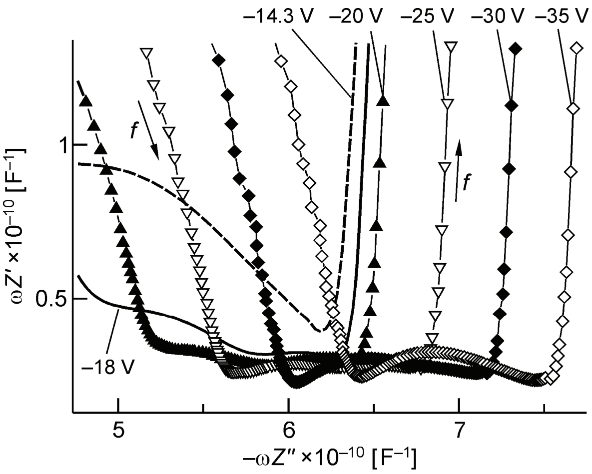

Fig. 5. Fragments of plots of the electric modulus in the complex plane. The reverse bias U_r values for which the measurements were performed are indicated in the figure

Conclusion

It is demonstrated that entrapping of the irradiation damaged layer by the space-charge region results in dramatic changes of the frequency dependences of a complex electric modulus. It was found that transformations of the complex plane plots of the electric modulus at the increased absolute values of reverse bias take place due to the change in the impedance ratio Z_L/Z_J of the irradiation damaged layer Z_L and space charge region Z_J as well as due to changes in the electron population of energy levels of the radiation defects.

This work has been carried out under financial support of the Belarusian Fundamental Research Fund (project F10D-002) and the German Academic Exchange Service DAAD

REFERENCES

[1] Lebedev A.A., Lebedev A.A., Davydov D.V., Capacitance measurements for diodes in the case of strong dependence of the diode-base series resistance on the applied voltage, *Semiconductors*, 34 (2000), No. 1, 115-118

[2] McPherson M., Capacitive effects in neutron-irradiated silicon diodes, *Nuclear Instruments and Methods in Physics Research Section A,* 488 (2002), n.1-2, 100-109

[3] McPherson M., Fermi level pinning in irradiated silicon considered as a relaxation-like semiconductor, *Physica B*, 344 (2004), No. 1-4, 52-57

[4] Emel'yanov A.M., Sobolev N.A., Yakimenko A.N., Capacitance-voltage characteristics of *p–n* structures based on (111) Si doped with erbium and oxygen, *Semiconductors,* 35 (2001), No. 3, 316-320

[5] Saadoune A., Dehimi L., Sengouga N., McPherson M., Jones B.K., Modelling of semiconductor diodes made of high defect concentration, irradiated, high resistivity and semi-insulating material: The capacitance-voltage characteristics, *Solid State Electron*, 50 (2006), No. 7-8, 1178-1182

[6] Dehimi L., Sengouga N., Jones B.K., Modelling of semiconductor diodes made of high defect concentration, irradiated, high resistivity and semi-insulating material: the current-voltage characteristics, *Nuclear Instruments and Methods in Physics Research Section A,* 519 (2004), No. 3, 532-544

[7] Dehimi L., Sengouga N., Jones B.K., Modelling of semiconductor diodes made of high defect concentration, irradiated, high resistivity and semi-insulating material: the internal field, *Nuclear Instruments and Methods in Physics Research Section A,* 517 (2004), No. 1-3, 109-120

[8] Process Wizard – 1D, version 1.3, Dawn Technologies, Inc.; (1999)

[9] Ziegler J.F., SRIM-2003, *Nuclear Instruments and Methods in Physics Research Section B,* 219-220 (2004), 1027-1036

[10] Barsoukov E., Macdonald J.R., Impedance spectroscopy: Theory experiment and applications, New York, Wiley, (2005), 595 p.

[11] Poklonski N.A., Gorbachuk N.I., Shpakovski S.V., Lastovskii S.B., Wieck A., Equivalent circuit of silicon diodes subjected to high–fluence electron irradiation, *Technical Physics*, 55 (2010), No. 10, 1463-1471

[12] Chelyadinskii A.R., Komarov F.F., Defect-impurity engineering in implanted silicon, *Physics-Uspekhi*, 46 (2003), No. 8, 789-820

[13] Milnes A.G., Deep impurities in semiconductors. New York, Wiley, (1973)

Authors: *prof. Nikolai A. Poklonski, dr Nikolay I. Gorbachuk, Anna V. Ermakova, dr Mariya I. Tarasik, Biaoruski Państwowy Uniiwersytet w Mińsk, ul. Prospekt Nezavisimosti 4, 220030, Minsk, Białoruś, E-mail: poklonski@bsu.by;*

Sergey V. Shpakovski, Viktor A. Filipenia, JSC Integral, ul. Korzhenevskogo 12, Mińsk, 220108, Białoruś, E-mail: shpaks@tut.by;

prof. Viktor A. Skuratov, Zjednoczony Instytut Badań Jądrowych, ul. Joliot - Curie 6, 141980 Dubna, Moskwa, Rosja, E-mail: skuratov@jinr.ru;

prof. Andreas Wieck, Rurski Uniwersytet, Bochum, ul. Universitaets 150, 44780 Bochum, Niemcy

dr inż. Tomasz N. Kołtunowicz, Politechnika Lubelska, Katedra Urządzeń Elektrycznych i Techniki Wysokich Napięć ul. Nadbystrzycka 38d, 20-618 Lublin, Polska, E-mail: t.koltunowicz@pollub.pl.